

An Additive Multilevel Preconditioning Method

Nathalie Marco, Bruno Koobus, Alain Dervieux

► **To cite this version:**

Nathalie Marco, Bruno Koobus, Alain Dervieux. An Additive Multilevel Preconditioning Method. [Research Report] RR-2310, INRIA. 1994. <inria-00074363>

HAL Id: inria-00074363

<https://hal.inria.fr/inria-00074363>

Submitted on 24 May 2006

HAL is a multi-disciplinary open access archive for the deposit and dissemination of scientific research documents, whether they are published or not. The documents may come from teaching and research institutions in France or abroad, or from public or private research centers.

L'archive ouverte pluridisciplinaire **HAL**, est destinée au dépôt et à la diffusion de documents scientifiques de niveau recherche, publiés ou non, émanant des établissements d'enseignement et de recherche français ou étrangers, des laboratoires publics ou privés.

INSTITUT NATIONAL DE RECHERCHE EN INFORMATIQUE ET EN AUTOMATIQUE

*An Additive Multilevel
Preconditioning Method*

Nathalie MARCO, Bruno KOOBUS and Alain DERVIEUX

N° 2310

Août 1994

PROGRAMME 6

Calcul scientifique,
modélisation
et logiciel numérique



*Rapport
de recherche*

1994

An Additive Multilevel Preconditioning Method

Nathalie MARCO, Bruno KOOBUS and Alain DERVIEUX

Programme 6 — Calcul scientifique, modélisation et logiciel numérique
Projet Sinus

Rapport de recherche n° 2310 — Août 1994 — 35 pages

Abstract: This paper describes a new approach of the Multilevel method studied in [4] and [11], in order to solve the 2D Laplace equation. The first approach of the multilevel method is a multiplicative or serial method since each level is addressed sequentially ; it presents, as MG methods, a mesh-independent convergence rate. It is more costly than MG methods, but easier to implement. In order to smooth all the frequency components of the error, the V-cycle strategy is used and it results in several cost functional evaluations per cycle.

In this paper, the proposed strategy is based on an additive approach. A preconditionner is deduced from this multilevel method, which provides a better efficiency than the previous method since all frequencies are addressed at the same time, while only one optimization iteration is needed. Furthermore, this method still presents a mesh-independent convergence rate.

(Résumé : tsvp)

Un Préconditionnement Additif issu de la Méthode Multi-niveau

Résumé : Dans ce papier, nous introduisons une nouvelle approche de la méthode Multi-niveau étudiée dans [4] et [11] pour résoudre l'équation de Poisson en 2D. La première approche est une méthode multiplicative traitant les niveaux les uns après les autres, qui présente, comme la méthode Multigrille, une convergence indépendante du maillage ; cette méthode Multi-niveau est plus coûteuse que la méthode Multigrille, mais elle est plus facile à implémenter. Dans le but de lisser toutes les fréquences de l'erreur, la stratégie V-cycle est utilisée et plusieurs évaluations par cycle de la fonctionnelle coût sont nécessaires.

Dans ce papier, la stratégie proposée est basée sur une approche additive. Un préconditionneur est déduit de la méthode Multi-niveau, ce qui permet d'obtenir un coût plus faible que celui de la méthode précédente étant donné que toutes les fréquences sont traitées dans la même itération d'optimisation. En outre, cette méthode présente encore une convergence indépendante du maillage.

Contents

1	Introduction	4
2	Additive Multilevel Method	6
2.1	Descent direction	7
2.1.1	Preamble	7
2.1.2	A descent direction	9
2.2	Symmetric preconditioning	11
3	Two-Grid Fourier analysis	12
4	Abstract convergence theory	18
4.1	Abstract theory	18
4.2	Verification of the main assumptions	22
5	Numerical experiments	24
5.1	Residual convergence	24
5.2	Mesh-Independent Convergence Rate	25
5.3	AMLP method applied to Optimum Design inverse Problem	26
6	Concluding remarks	31
	Bibliographie	35

1 Introduction

The focus of this work is to study a multilevel optimization algorithm. For theoretical analysis, we concentrate on the 2-D Poisson equation model with homogeneous Dirichlet conditions, solved when minimizing a quadratic cost functional with a basic relaxation process of the form :

$$U \leftarrow U - \rho B^{-1}(AU - b) \quad (1)$$

where $\rho B^{-1}(AU - b)$ is the correction term, B^{-1} is the preconditioning and $AU - b$ is the gradient of the cost functional $J(U)$. Three different ways in applying a multilevel approach can be observed :

Method 1 : in [4] and [11], a multilevel method is used with a V-cycle strategy which consists of iterating (1) from the finest level to the coarsest one and to return on the finest one (one sawtooth V-cycle), until convergence to zero of the correction term. The algorithm is :

$$U \leftarrow U - \rho(AU - b) \quad \text{on the fine level} \quad (B^{-1} = Id) \quad (2)$$

and

$$U \leftarrow U - \rho PP^*(AU - b) \quad \text{on the coarse level} \quad (B^{-1} = PP^*) \quad (3)$$

This is a multiplicative method, since the different levels are considered successively, the initialization on a definite level being the calculated solution on the previous level. The complexity of such a method is $O(N(\log N)^2)$, because the residual (“cost functional”) is always computed on the finest level.

Method 2 : another approach to solve (1) consists of an additive multilevel method. On each level, the correction term is implemented with the same initialization and on the finest level, the correction term is the sum of the ones calculated on coarse levels. The algorithm can be written as follows (with two levels) :

$$U \leftarrow U - \rho((AU - b)_{H.F} + (AU - b)_{L.F}) \quad (4)$$

where $(AU - b)_{H.F}$ has been completely calculated on the fine level (H.F. : high frequencies) when solving (2) and $(AU - b)_{L.F}$ has been completely calculated

on the coarse level (L.F. : low frequencies) when solving (3). This additive approach is used for a multigrid method in [7] with residual splitting, which is the main idea of Chan and Tuminaro in [2] who implement a parallel MG algorithm.

In the case of the optimization problem, two descent directions are built on the fine and coarse levels. However, the optimal step-length ρ has to be calculated for the optimization algorithm (4) ; as the two descent directions are both weighted by 1, their sum should no more be a good descent direction for the algorithm. The remedy is then to weight each descent direction by a step-length relaxation : the coarser the level is, the larger step-length is, to be able to attack low frequencies. It is the subject of *Method 3*.

Method 3 : in the sequel, we introduce an additive multilevel method in which all the levels are swept in one optimization iteration. The correction term is decomposed as follows :

$$\rho(AU - b) = \rho \sum_{i=finest}^{coarsest} \rho_i(AU - b)_i \quad (5)$$

There is only one seek of the descent step ρ and one implementation of the cost functional for all the levels. The ρ_i 's depend on the levels and are fixed with a 2-Grid Fourier analysis. This method is less costly than the two previous ones ; its complexity is about $O(N \log N)$. The correction terms are totally independent of each other, which allows to treat them at the same time. As all the frequencies are taken into account simultaneously and as we have a unique descent direction and a unique residual for all the levels, it is possible to conjugate the descent direction, which was rather hard for *Method 1*.

In Section 2, we present the additive multilevel preconditioning method ; we demonstrate that the correction term is a descent direction and that the preconditioning can be built symmetric. In Section 3, we set a 2-Grid Fourier analysis which brings informations about the steps ρ_i 's in order to get a stable scheme. In Section 4, we carry a mesh-independent convergence proof for a 2-grid additive abstract algorithm. The proof has been inspired by H. Guillard in [6] : the mesh-independent convergence rate was demonstrated for multilevel method with V-cycle strategy on non embedded abstract spaces. The idea of

Guillard was to split the original space in a direct sum of subspaces. In Section 5, we present numerical experiments for the Poisson problem. We present also an attempt to use AMLP (Additive Multilevel Preconditioning) method in the case of the optimization of a nozzle in a 2D Euler flow (see [10]) ; firstly, the method is used with complete solution of state and adjoint-state equations and secondly, it is combined with one-shot method.

2 Additive Multilevel Method

To fix the ideas, it will be useful to think about the following model problem :

$$\begin{cases} -\Delta U = b & \text{on } \Omega \\ U|_{\Gamma} = 0 & \text{on } \delta\Omega \end{cases} \quad (6)$$

Let J be a real-valued functional defined on a Hilbert E . We consider the optimization problem :

$$\text{Find } \bar{U} \text{ such that : } J(\bar{U}) = \min_{U \in E} J(U) \quad (7)$$

i.e., $E = H_0^1(\Omega)$, Ω is a regular domain of \mathbb{R}^2 and :

$$J(U) = \frac{1}{2} \langle AU, U \rangle - \langle b, U \rangle \quad (\langle \cdot, \cdot \rangle \text{ is the scalar product in } E) \quad (8)$$

Its gradient (in the Fréchet sense) is of the form :

$$\nabla J(U).U = \langle AU - b, U \rangle = G(U).U \quad (9)$$

Let $(E_i)_{1 \leq i \leq n}$ be a scale of embedded subspaces of E :

$$E = E_0 \supset E_1 \supset \cdots E_i \supset \cdots E_n$$

We construct the following iterative algorithm :

$$\begin{cases} U^0 \text{ given} \\ U^{\alpha+1} = U^\alpha - \rho \sum_{i=finest}^{coarsest} \Pi_i G(U^\alpha) \end{cases} \quad (10)$$

Π_i are orthogonal projections from the finest level to the level i (level 1 being by convention the finest level and level n being the coarsest one) :

$$\Pi_i = \rho_i P_i^1 (P_1^i)^* \quad (\rho_i > 0 \quad \forall i) \quad (11)$$

All the frequencies are affected, independently of each other. The decomposition allows only one estimation of the gradient and the cost functional, for an optimization iteration. The complexity is then lower than the one of the multilevel method with V-cycle strategy (*Method 1*) : computation of the cost functional on fine level is $O(N \log N)$ and the effort in preconditioning the gradient by an operator depending on all the levels gives another $O(N \log N)$.

Algorithm (10) can be written as :

$$\begin{cases} U^0 & \text{given} \\ U^{\alpha+1} = U^\alpha - \rho \sum_{i=1}^n \rho_i g_i(U^\alpha) \end{cases} \quad (12)$$

Each $\rho_i g_i(U^\alpha)$ is a descent direction on level i , n is the number of levels and the ρ_i 's are steps-length relaxation on each level. By a Fourier analysis presented in Section 3, the ρ_i 's will be fixed in order to obtain a stable scheme. ρ is the descent step of the method ($\rho > 0$) and $\sum_{i=1}^n \rho_i g_i(U^\alpha)$ is the descent direction on the finest level.

Remark : the coarser the level i is, the larger ρ_i is. The coarseness of a level describes low frequencies ; then, the step-length relaxation has to be large to be able to attack these frequencies. We get the following inequalities :

$$0 < \rho_1 < \rho_2 < \dots < \rho_n \quad (13)$$

2.1 Descent direction

2.1.1 Preamble

It has been observed that simplicial Galerkin approximations are equivalent in some sense to ad-hoc finite volume formulations on specific dual meshes. For two-dimensional case, the dual mesh is derived when joining middles of

adjacent sides of each node A_i with centroids of triangles where A_i is a vertex. A partition is then defined as :

$$\Omega_h = \bigcup_{i=1, \dots, n_h} \mathcal{C}_i, \quad n_h \text{ is the fine level nodes number.} \quad (14)$$

\mathcal{C}_i is the resulting cell, or control volume. On the finest level, there are as many cells as nodes. Coarse levels are obtained by the agglomeration of control volumes represented on Figure 1. The optimization problem is solved on unstructured meshes (or dual meshes).

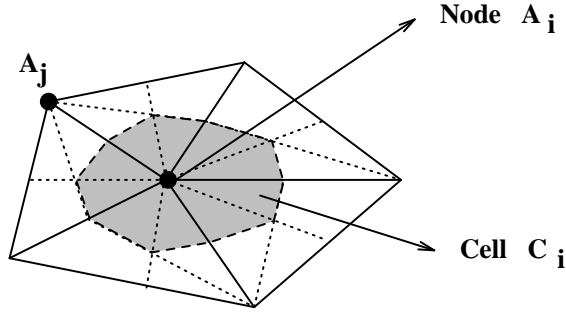


Figure 1: $Cell \mathcal{C}_i$.

Let us recall briefly the definitions of the transfer operators P and P^* between two levels.

The discrete fine level is a Hilbert space, V_h , and the coarse discrete one is another Hilbert space, V_{2h} , with $V_{2h} \subset V_h$:

$$V_h = \{\varphi_i, i = 1 \dots n_h / \text{P1 Galerkin functions}\}$$

$$V_{2h} = \{\Phi_J, J = 1 \dots n_{2h} / \Phi_J = \sum_{i \in I_J} \varphi_i\} \quad \text{where } I_J \text{ is defined by :}$$

If I^f is the set of fine indices i and n_h is its cardinal number, then,

$$I^f = \{1, \dots, i, \dots, n_h\} = I_1 \cup \dots \cup I_J \cup \dots \cup I_{n_{2h}} \quad (n_{2h} \ll n_h) \quad (15)$$

V_h is equipped by the following scalar product :

$$\forall (u_h, v_h) \in V_h^2 \quad (u_h, v_h)_h = \sum_i^{n_h} (u_h)_i (v_h)_i \text{Area}(i) \quad (i \text{ is a cell}) \quad (16)$$

P is the linear prolongation operator from V_{2h} to V_h and it is a canonical injection :

$$\forall u_{2h} \in V_{2h} \quad Pu_{2h} = u_{2h} \in V_h \quad (17)$$

P^* is the restriction operator from V_h to V_{2h} , and it is defined via P as its adjoint from the previous scalar product (see [4] and [11]) by :

$$(P^*u_h)_j = \frac{\sum_{j_m \subset j}^{n_h} (u_h)_{j_m} \mathcal{A}rea(j_m)}{\mathcal{A}rea(j)} \quad (18)$$

j is a coarse cell, j_m are fine cells included in j .

Remarks : In practice, for the i -th level, P and P^* are defined as follows :

$$P = P_2^1 \circ P_3^2 \circ \dots \circ P_i^{i-1} \quad \text{and} \quad P^* = (P_{i-1}^i)^* \circ \dots \circ (P_2^3)^* \circ (P_1^2)^*$$

2.1.2 A descent direction

- When using **two** levels, algorithm (12) becomes :

$$U^{\alpha+1} = U^\alpha - \rho \left[\rho_1 (Id - P_2^1 (P_1^2)^*) G(U^\alpha) + \rho_2 P_2^1 (P_1^2)^* G(U^\alpha) \right] \quad (19)$$

$$= U^\alpha - \rho \left[\rho_1 G(U^\alpha) + (\rho_2 - \rho_1) P_2^1 (P_1^2)^* G(U^\alpha) \right] \quad (20)$$

$\rho_1 (Id - P_2^1 (P_1^2)^*) G(U^\alpha)$ denotes the high frequencies components of the residual and $\rho_2 P_2^1 (P_1^2)^* G(U^\alpha)$ denotes the low frequencies components of the residual.

Lemma 2.1 *Algorithm (20) is a descent method for the optimization problem (7), i.e.,*

$$J(U^{\alpha+1}) \leq J(U^\alpha) \quad (21)$$

Proof :

From Taylor formula, we have :

$$J(U + V + P_2^1 W) = J(U) + \langle G(U), V \rangle_{V_h} + \langle G(U), P_2^1 W \rangle_{V_h} + O(V + W)$$

Let ρ , ρ_1 and ρ_2 be reals strictly positive, $V = -\rho\rho_1 G(U) \in V_h$ and $W = -\rho(\rho_2 - \rho_1)(P_1^2)^* G(U) \in V_{2h}$. We obtain :

$$\begin{aligned} J(U + V + P_2^1 W) = & J(U) - \rho \left(\rho_1 < G(U), G(U) >_{V_h} \right. \\ & \left. - (\rho_2 - \rho_1) < (P_1^2)^* G(U), (P_1^2)^* G(U) >_{V_{2h}} + O(\rho_2 - \rho_1) \right) \end{aligned}$$

As inequality (13) leads the fact that $\rho_2 - \rho_1 > 0$, we deduce that :

$$J(U^{\alpha+1}) \leq J(U^\alpha). \quad \square$$

- When using **three** levels, algorithm (12) becomes :

$$\begin{aligned} U^{\alpha+1} = U^\alpha - \rho \left[\rho_1 G(U^\alpha) + (\rho_2 - \rho_1) P_2^1 (P_1^2)^* G(U^\alpha) \right. \\ \left. + (\rho_3 - \rho_2) P_2^1 P_3^2 (P_2^3)^* (P_1^2)^* P_2^1 (P_1^2)^* G(U^\alpha) \right] \end{aligned} \quad (22)$$

The proof is the same as the previous one.

- When using **n** levels, notations are harder, but the proof is the same as the one with two levels.

When setting $\sum_{i=1}^n \rho_i g_i(U^\alpha) = Res^\alpha$, the optimal step-length ρ is the step which minimizes :

$$J(U^\alpha - \rho Res^\alpha) = \frac{1}{2} \rho^2 < A Res^\alpha, Res^\alpha > - \rho < G(U^\alpha), Res^\alpha > + J(U^\alpha) \quad (23)$$

$$\iff \rho_{opt} = \frac{< G(U^\alpha), Res^\alpha >}{< A Res^\alpha, Res^\alpha >} \quad (24)$$

Remark : when substituting ρ_{opt} in (23), we obtain :

$$J(U^{\alpha+1}) - J(U^\alpha) = -\frac{1}{2} \frac{< G(U^\alpha), Res^\alpha >^2}{< A Res^\alpha, Res^\alpha >} < 0 \quad \forall \alpha$$

A more general lemma is then derived :

Lemma 2.2 *Algorithm (12) is a descent method for the optimization problem (7) and the optimal step-length ρ_{opt} is given by (24).*

In the next section, we prove that the preconditioning is symmetric.

2.2 Symmetric preconditioning

The iterative algorithm (12) can be transformed as :

$$U^{\alpha+1} = U^\alpha - \rho B^{-1} G(U^\alpha) \quad (25)$$

- When using two levels,

$$B^{-1} = \rho_1 Id + (\rho_2 - \rho_1) P_2^1 (P_1^2)^*,$$

It clearly implies that ${}^t(B^{-1}) = B^{-1}$.

- When using three levels,

$$B^{-1} = \rho_1 Id + (\rho_2 - \rho_1) P_2^1 (P_1^2)^* + (\rho_3 - \rho_2) P_2^1 P_3^2 (P_2^3)^* (P_1^2)^* P_2^1 (P_1^2)^*$$

The two first terms are symmetric.

Lemma 2.3 *The third term $P_2^1 P_3^2 (P_2^3)^* (P_1^2)^* P_2^1 (P_1^2)^*$ is a symmetric operator.*

Proof :

$P_2^1 P_3^2 (P_2^3)^* (P_1^2)^* P_2^1 (P_1^2)^*$ is symmetric if :

$$P_3^2 (P_2^3)^* (P_1^2)^* P_2^1 = (P_1^2)^* P_2^1 P_3^2 (P_2^3)^*$$

The matricial representation of operator P_{i+1}^i is a $n_i \times n_{i+1}$ matrix and the one of operator $(P_i^{i+1})^*$ is a $n_{i+1} \times n_i$ matrix.

Note that $n_1 > n_2 > \dots > n_i > n_{i+1}$ (n_i is the nodes number of level i).

With the above definitions of P and P^* , we deduce that :

$P_{i+1}^i (P_i^{i+1})^*$ is a $n_i \times n_i$ symmetric matrix and $(P_{i-1}^i)^* P_i^{i-1}$ is a $n_i \times n_i$ diagonal matrix.

Then,

$$(P_{i-1}^i)^* P_i^{i-1} P_{i+1}^i (P_i^{i+1})^* = K \times Id \times (\text{symmetric}) = K \times (\text{symmetric})$$

$$P_{i+1}^i (P_i^{i+1})^* (P_{i-1}^i)^* P_i^{i-1} = (\text{symmetric}) \times K \times Id = K \times (\text{symmetric}) \quad (K \in \mathbb{R})$$

$P_2^1 P_3^2 (P_2^3)^* (P_1^2)^* P_2^1 (P_1^2)^*$ is symmetric. \square

We conclude that B^{-1} is symmetric.

- When using n levels, the form of B^{-1} is too difficult to be written ; we note that it is the composition of matrices of previous type and symmetric matrices of type

$$P_{i+1}^i P_{i+2}^{i+1} \cdots (P_{i+1}^{i+2})^* (P_i^{i+1})^*,$$

the representation of which is on Figure 2. They are diagonal block matrices.

Figure 2 shows two matrices, C and K, represented as block matrices. Matrix C is a 2x2 block matrix with blocks of size n_i . The top-left and bottom-right blocks are labeled '1', and the top-right and bottom-left blocks are labeled '0'. Matrix K is a block tridiagonal matrix with blocks of size n_i and 2×2 blocks. The top-left block is labeled '1', and the bottom-right block is labeled '1'. The blocks are arranged in a diagonal pattern, with '0' blocks in the off-diagonal positions. The dimensions are indicated by arrows: n_i for the height and width of the main blocks, and 2 for the height and width of the small blocks.

Figure 2: Sketch of matrices $P_{i+1}^i P_{i+2}^{i+1} \cdots (P_{i+1}^{i+2})^* (P_i^{i+1})^*$ and matrices $P_{i+1}^i (P_i^{i+1})^*$

B^{-1} is then a symmetric matrix. Note that B^{-1} does not depend on U . B^{-1} is a hierarchical linear preconditioning.

In the following section, a Two-Grid Fourier analysis is developed in order to evaluate which steps-length relaxation on coarse levels will provide a stable scheme.

3 Two-Grid Fourier analysis

We study here an analysis which can be applied to general multigrid algorithms on regular grids. However, since the complexity of the analysis increases dramatically with the number of levels, we restrict the study to the analysis of a 2-Grid scheme and we give some important features which have to be taken into account to insure its efficiency. The study is focused in 1-D.

The relaxation method we use is a steepest method in which all levels are considered simultaneously. The purpose of the two-grid Fourier analysis consists of building the amplification factor $G(\Theta)$ which corresponds to the Fourier symbol of the iterative operator. We pay a particular attention to the highest frequency modes (corresponding to the components having the smallest wavelength with respect to the fine mesh size). The highest frequencies are generally defined to be those belonging to the interval $[\frac{\Pi}{2}, \Pi]$. A good smoother should ideally damp these frequencies such that after smoothing, the resulting error could be represented on a coarser discretization. Therefore, we are interested in $\min_{\Theta \in [\frac{\Pi}{2}, \Pi]} |G(\Theta)|$ as a function of a parameter ρ (relaxation parameter).

In fact, as we have two relaxation parameters (ρ_1 on the fine grid and ρ_2 on the coarse one), we are going to fix ρ_1 , and ρ_2 will be the parameter ρ defined in the previous sentence.

Since, we only work with two levels, a non approximate Fourier analysis can be applied (see [5]) ; we proceed as Couaillier-Peyret in [3] and Leclercq-Stoufflet in [8]. This kind of Fourier analysis consists of splitting the Fourier modes in two parts, to distinguish from those corresponding to the even nodes to those associated with the odd nodes. Thus, we are searching solutions (U_h^n, V_h^n) defined on each node, of the following form :

$$\begin{cases} (U_h^n)_{2j} = (\hat{U}_h^n)_k \exp^{i(2j)(\Theta_h)_k} \\ (V_h^n)_{2j+1} = (\hat{V}_h^n)_k \exp^{i(2j+1)(\Theta_h)_k} \end{cases} \quad (26)$$

with :

$$(\hat{U}_h^0)_k = (\hat{V}_h^0)_k$$

The phase angle is $(\Theta_h)_k = \frac{2\Pi k}{n_h}$, where $0 \leq k < n_h$ and n_h is the number of discretized points. h is the spatial discretization step on the fine grid.

The Laplace Equation is considered on the unit circle ($0 \equiv 2\Pi$) and a centered spatial discretization is chosen together with an explicit first-order relaxation iteration. In the following, we will note the relaxation iteration by "n" :

$$(U_h^{n+1})_i = (U_h^n)_i - (D^{-1})_i \rho B^{-1} G((U_h^n)_i) \quad (27)$$

where D^{-1} is the inverse of diagonal of matrix A , $(D^{-1})_i = \frac{h^2}{2}$, and ρ is the relaxation step. The discretized form of $G((U_h^n)_i)$ is :

$$G((U_h^n)_i) = (AU_h^n)_i - b_i = \frac{-(U_h^n)_{i+1} + 2(U_h^n)_i - (U_h^n)_{i-1}}{h^2} - b_i$$

This defines an iterative process $(U_h^{n+1}) = f(U_h^n)$ which converges to a stationary point.

Notations : to define the transfer operators, h subscripts will be used to denote quantities on the fine level, while $2h$ subscripts will hold for coarse level.

$$(P^*U_h)_j = \frac{(U_h)_{2j} + (U_h)_{2j+1}}{2}$$

$$(PU_{2h})_{2j} = (U_{2h})_j$$

$$(PP^*U_h)_{2j} = \frac{(U_h)_{2j} + (U_h)_{2j+1}}{2} = (PP^*U_h)_{2j+1}$$

With the multilevel method, as we always work on the fine level, it will not be necessary, in the sequel, to use the h subscript for solution (U_h^n, V_h^n) .

When considering the discretized error of the scheme $e^n = \bar{U} - U^n$, (27) becomes :

$$e_i^{n+1} = e_i^n - D^{-1} \rho B^{-1} A e_i^n \quad (28)$$

(\bar{U} is the exact solution of Laplace equation : $\bar{U} = A^{-1}b$).

We do not more use the RHS. However, we will keep the same notations as previously, i.e., (U^n, V^n) , even and odd components of the error e^n .

In [4] and [11], multilevel method with V-cycle strategy was considered with and without a “smoothing” operator of the form :

$$(LU)_i = (1 - \theta)U_i + \theta \frac{\sum_{j \in \mathcal{N}(i) \cup \{i\}} \mathcal{A}_j U_j}{\sum_{j \in \mathcal{N}(i) \cup \{i\}} \mathcal{A}_j} \quad (29)$$

where \mathcal{A}_j is the area of cell \mathcal{C}_j , $\mathcal{N}(i)$ represents the neighbors of node i and θ is the smoothing parameter. For an accurate value of θ ($\theta = \frac{3}{4}$ in 1D theory and $\theta = 1$, from 2D numerical experiment ; see [9]), the minimization problem was V-consistent and it implied a mesh-independent convergence rate (i.e. solution on coarse level is a good approximation of solution on fine level).

The two-Grid Fourier analysis is going to be applied first of all on the problem without smoothing :

$$e^{n+1} = e^n - D^{-1} \left[\rho_1 (Id - PP^*)Ae^n + \rho_2 PP^*Ae^n \right] \quad (30)$$

and after on the problem with smoothing :

$$e^{n+1} = e^n - D^{-1} \left[\rho_1 (Id - LPP^*L^*)Ae^n + \rho_2 LPP^*L^*Ae^n \right] \quad (31)$$

• Two-Grid Fourier analysis applied on problem (30) :

$$e_i^{n+1} = e_i^n - \frac{h^2}{2} \left[\rho_1 (Ae^n)_i + (\rho_2 - \rho_1)(PP^*Ae^n)_i \right] \quad (32)$$

In Appendix 1, even and odd components of the error are calculated, in terms of ρ_1 and ρ_2 , and, when using Fourier modes as defined in (26), the amplification matrix $G(\Theta_k, \rho_1, \rho_2)$ is given.

As ρ_1 has to be fixed, let us consider the monogrid Fourier analysis. Schemes (30) and (31) become :

$$e_i^{n+1} = e_i^n - D^{-1} \rho Ae_i^n \quad \text{when taking } \rho_2 = \rho_1 = \rho \text{ and } B^{-1} = Id$$

and the amplification matrix is :

$$\begin{pmatrix} \hat{U}_k^{n+1} \\ \hat{V}_k^{n+1} \end{pmatrix} = \begin{pmatrix} 1 - \rho & \rho \cos \Theta_k \\ \rho \cos \Theta_k & 1 - \rho \end{pmatrix} \begin{pmatrix} \hat{U}_k^n \\ \hat{V}_k^n \end{pmatrix}$$

The stability of the scheme is depicted on Figure 3 where the reduction factor (maximum of the two eigenvalues) is function of Θ_k , $0 < \Theta_k < \Pi$. Note that for $\rho = 1$, we observe a good stability.

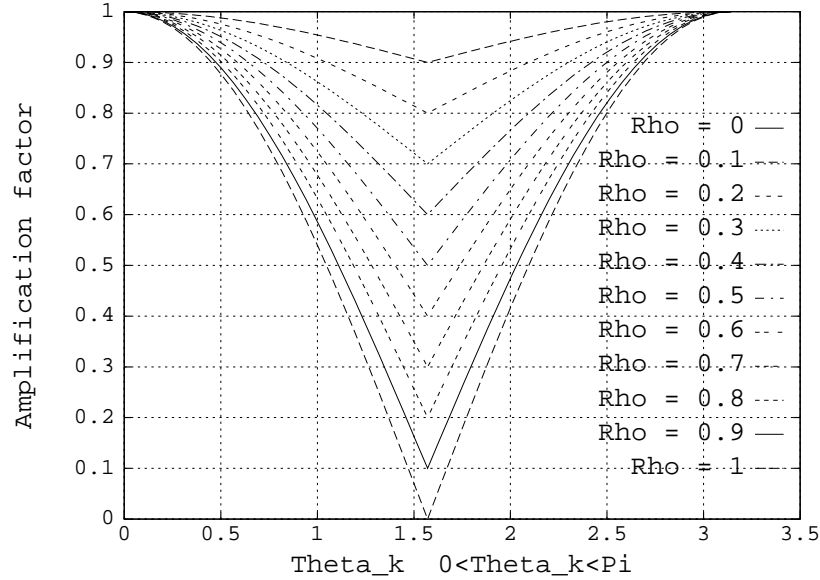


Figure 3: *Monogrid Fourier analysis.*

As ρ_1 is the step-length relaxation associated to the fine grid (monogrid), we fix $\rho_1 = 1$ (the optimal one by Monogrid Fourier analysis), and only ρ_2 varies. Figure 4 describes the stability of the scheme, according to values of ρ_2 .

- Two-Grid Fourier analysis applied on problem (31) :

$$e_i^{n+1} = e_i^n - \frac{h^2}{2} \left[\rho_1 (Ae^n)_i + (\rho_2 - \rho_1) (LPP^* L^* Ae^n)_i \right] \quad (33)$$

In Appendix 2, even and odd components of the error are given. We also exhibit the amplification matrix $G(\Theta_k, \rho_1, \rho_2)$.

As in the two-grid Fourier analysis without smoothing, we fix $\rho_1 = 1$ and ρ_2 varies. Figure 5 depicts the stability of the scheme. We note that for a ρ_2 four times greater, the scheme is still stable. For a ρ_2 five times greater, we are at the limit of the stability.

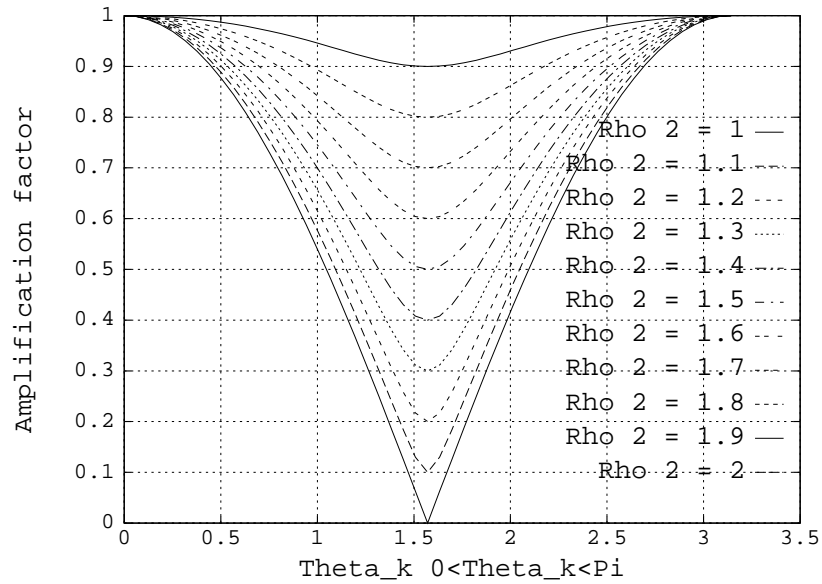


Figure 4: *Two-Grid Fourier analysis without smoothing.*

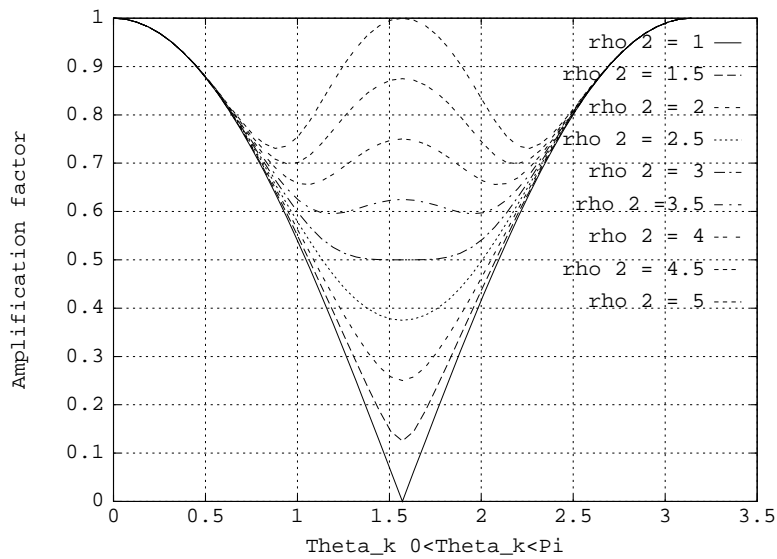


Figure 5: *Two-Grid Fourier analysis with smoothing.*

We conclude that, without smoothing, there is the following relation for the steps relaxation ρ_i :

$$\left\{ \begin{array}{l} \rho_1 = 1 \\ \rho_i = 2^{i-1}\rho_1 \quad i > 1 \end{array} \right.$$

while with smoothing, the relation is :

$$\begin{cases} \rho_1 = 1 \\ \rho_i = 4^{i-1}\rho_1 \text{ or } \rho_i = 5^{i-1}\rho_1 \end{cases}$$

4 Abstract convergence theory

We now present a proof for the 2-grid additive multilevel algorithm. A similar proof for a 2-grid parallel multigrid algorithm is shown in [7]. Our proof was inspired by the previous one.

4.1 Abstract theory

Let V be the vectorial space of functions u defined on Ω , open bounded domain in \mathbb{R}^2 . We assume that V is a Hilbert space, supplied by the scalar product $\langle \cdot, \cdot \rangle$. When considering the linear operator A defined on V , continuous, self-adjoint and positive definite in the following meaning :

$$\langle Au, u \rangle \geq 0, \forall u \in V$$

$$\langle Au, u \rangle = 0 \Rightarrow u = 0$$

we define a new scalar product noted $\langle \cdot, \cdot \rangle_A$ by :

$$\forall u \in V, \langle u, u \rangle_A = \langle Au, u \rangle$$

Let b be a given function in V , then the problem

$$\begin{cases} \text{Find } u \text{ in } V \text{ such that} \\ Au = b \end{cases}$$

has a unique solution $\bar{u} = A^{-1}b$.

Let suppose that Ω_h is a discretization of Ω , and V_h , the discrete space, is dense in V . Let A_h be the discrete operator in V_h . The initial problem restricted to V_h becomes :

$$\begin{cases} \text{Find } u_h \text{ in } V_h \text{ such that} \\ A_h u_h = b_h \end{cases}$$

It has a unique solution $\bar{u}_h = A_h^{-1}b_h$.

To be more explicit and to have similar notations with Multigrid method, we rename the transfer operators P and P^* by I_H^h and I_h^H (H represents the spatial discretization step on coarse level).

Let consider the splitting operator T_h , defined on V_h , which reaches high frequencies components and an other splitting operator $S_h = Id_h - T_h$, from V_h to the kernel of T_h , which reaches low frequencies components :

$$T_h = Id_h - I_H^h I_h^H \quad (34)$$

$$S_h = I_H^h I_h^H \quad (35)$$

We then have the following decomposition :

$$V_h = Im(T_h) \oplus Im(S_h)$$

Assumption 1 : S_h and T_h are orthogonal projection operators.

Let \bar{T}_h and \bar{S}_h be another splitting operators defined by :

$$\bar{T}_h = A_h^{-1}T_h A_h \quad \text{and} \quad \bar{S}_h = A_h^{-1}S_h A_h$$

Assumption 2 : \bar{T}_h and \bar{S}_h are orthogonal projection operators.

Algorithm :

1. $n \leftarrow 0$
 $\varepsilon = 10^{-10}$
2. $u_h^{n+1} = u_h^n - \rho \left[\alpha_h \bar{T}_h T_h (A_h u_h^n - b_h) + \alpha_H \bar{S}_h S_h (A_h u_h^n - b_h) \right]$
 $= u_h^n - \rho B^{-1}G(u_h^n)$
3. **if** $\|B^{-1}G(u_h^n)\| \leq \varepsilon$ **goto** 4 **else** $n \leftarrow n + 1$ **goto** 2
4. **end**

ρ is a constant small enough ($\rho \ll 1$) and α_h and α_H are ρ_1 and ρ_2 defined in Section 3.

Remark : As the AMLP method is applied on an optimization problem, the optimization method we use is a *gradient method*, and operator A_h is defined as follows :

$$A_h : H_h \longrightarrow H'_h$$

where H_h is a Hilbert and H'_h is its dual space. The residual $A_h u_h - b_h = r_h$ (the gradient of cost functional J) belongs to the dual space. As part 2 of the above algorithm acts in the Hilbert H_h , we need a canonical isomorphism Λ_h acting from H'_h to H_h . Operators T_h and S_h are applied on the residual, they act in the dual space. From their definitions, operators \overline{T}_h and \overline{S}_h act in H_h . Then, part 2 of the Algorithm should be written :

$$u_h^{n+1} = u_h^n - \rho [\alpha_h \overline{T}_h \Lambda_h T_h r_h^n + \alpha_H \overline{S}_h \Lambda_h S_h r_h^n]$$

As the isomorphism is not necessary for the sequel of the proof, we will not use it. \square

The iterative error is given by : $e_h^n = \overline{u}_h - u_h^n$. Then, the algorithm becomes :

$$\begin{aligned} e_h^{n+1} &= e_h^n - \rho \alpha_h \overline{T}_h T_h A_h e_h^n - \rho \alpha_H \overline{S}_h S_h A_h e_h^n \\ &= M_h e_h^n \end{aligned} \tag{36}$$

$M_h = Id_h - \rho \alpha_h \overline{T}_h T_h A_h - \rho \alpha_H \overline{S}_h S_h A_h$ is the iterative operator of 2-grid additive algorithm. When applying to M_h orthogonal projection operators \overline{T}_h and \overline{S}_h , it follows that :

$$\begin{aligned} \overline{T}_h M_h &= \overline{T}_h (Id_h - \rho \alpha_h T_h A_h) = \overline{T}_h (Id_h - \rho \alpha_h A_h) \overline{T}_h \\ \overline{S}_h M_h &= \overline{S}_h (Id_h - \rho \alpha_H S_h A_h) = \overline{S}_h (Id_h - \rho \alpha_H A_h) \overline{S}_h \end{aligned}$$

Then, equation (36) can be written in the following way :

$$\begin{aligned} e_h^{n+1} &= \overline{T}_h M_h e_h^n + \overline{S}_h M_h e_h^n \\ &= \overline{T}_h (Id_h - \rho \alpha_h A_h) \overline{T}_h e_h^n + \overline{S}_h (Id_h - \rho \alpha_H A_h) \overline{S}_h e_h^n \end{aligned} \tag{37}$$

It finally implies that :

$$\|e_h^{n+1}\|^2 = \|\overline{T}_h(Id_h - \rho \alpha_h A_h)\overline{T}_h e_h^n\|^2 + \|\overline{S}_h(Id_h - \rho \alpha_H A_h)\overline{S}_h e_h^n\|^2 \quad (38)$$

As in [7], we assume two verified properties :

P1 : $\exists \alpha_1 \in]0, 1[$, such that $\forall e_h \in V_h$

$$\|\overline{T}_h(Id_h - \rho \alpha_h A_h)\overline{T}_h e_h^n\| \leq \alpha_1 \|\overline{T}_h e_h^n\| \quad (39)$$

where $\alpha_1 < 1$ is independent of h .

P2 : $\exists \alpha_2 \in]0, 1[$, such that $\forall e_h \in V_h$

$$\|\overline{S}_h(Id_h - \rho \alpha_H A_h)\overline{S}_h e_h^n\| \leq \alpha_2 \|\overline{S}_h e_h^n\| \quad (40)$$

where $\alpha_2 < 1$ is **dependent** of h (because it is not a 2-Grids-Ideal method but only a 2-Grids method).

These two properties express the contraction property for both high and low frequencies. We then can state the following proposition :

Proposition 4.1 *Under properties (39) and (40), the additive multilevel 2-grid algorithm is convergent :*

$$\exists \alpha \in]0, 1[, \text{ such that } \forall n , \|e_h^{n+1}\| \leq \alpha \|e_h^n\| \quad (41)$$

where $\alpha = \max(\alpha_1, \alpha_2)$ and :

$$\lim_{n \rightarrow +\infty} u_h^n = \overline{u}_h \quad (42)$$

Proof :

Equation (38) and hypothesis (39) and (40) imply that :

$$\begin{aligned} \|e_h^{n+1}\|^2 &\leq \alpha_1^2 \|\overline{T}_h e_h^n\|^2 + \alpha_2^2 \|\overline{S}_h e_h^n\|^2 \\ &\leq \max(\alpha_1^2, \alpha_2^2) \left(\|\overline{T}_h e_h^n\|^2 + \|\overline{S}_h e_h^n\|^2 \right) \\ &\leq \max(\alpha_1^2, \alpha_2^2) \|e_h^n\|^2 \end{aligned}$$

where $\text{Max}(\alpha_1, \alpha_2) = \alpha < 1$.

We finally obtain, by a recursive process :

$$\|e_h^{n+1}\|^2 \leq (\alpha^2)^n \|e_h^0\|^2$$

and :

$$\lim_{n \rightarrow +\infty} \|e_h^{n+1}\| \leq \lim_{n \rightarrow +\infty} (\alpha^n \|e_h^0\|) = 0$$

The series of general term e_h^n tends towards 0 in V_h when n tends towards $+\infty$.

We deduce that $\lim_{n \rightarrow +\infty} u_h^n = \bar{u}_h$. The error decreases with factor α . \square

Remark : Property 1 is an actual smoothing property : high frequencies are damped, α_1 does not depend on h . Property 2 concerns the coarse level with low frequencies. It is satisfied if its stationary point is an approximation of the one of the algorithm. This property verifies the consistency property announced in [11], for example ; the smooth part of the error decreases. If $\alpha_1 \leq \alpha_2$, then the two-level method converges as fast as the one-level method applied to the coarse level. This means that the convergence of a Multilevel method depends only on its coarsest level convergence. We then obtain a mesh-independent convergence rate.

4.2 Verification of the main assumptions

On a concrete example, let demonstrate that S_h and T_h are orthogonal projection operators :

As seen in the previous section,

$$\begin{aligned} (I_h^H u_h)_p &= \frac{(u_h)_{2p} + (u_h)_{2p+1}}{2} \\ (I_H^h u_H)_{i=2p} &= (u_h)_p = (I_H^h u_H)_{i=2p+1} \\ (I_H^h I_h^H u_h)_{i=2p} &= \frac{(u_h)_{2p} + (u_h)_{2p+1}}{2} = K_h = (I_H^h I_h^H u_h)_{i=2p+1} \end{aligned}$$

When composing another time by $I_H^h I_h^H$, we obtain :

$$[I_h^H (I_H^h I_h^H u_h)]_p = \frac{\frac{(u_h)_{2p} + (u_h)_{2p+1}}{2} + \frac{(u_h)_{2p} + (u_h)_{2p+1}}{2}}{2} = K_h$$

$$(I_H^h[I_H^H(I_H^h I_H^H u_h)])_{i=2p} = K_h = (I_H^h[I_H^H(I_H^h I_H^H u_h)])_{i=2p+1}$$

We then deduce that :

$$S_h S_h = S_h$$

An example of this equality has been derived on Figure 6. The operator $I_H^h I_H^H I_H^h I_H^H$ has been applied to a function $u(x, y)$ and $I_H^h I_H^H u(x, y)$ and $I_H^h I_H^H I_H^h I_H^H u(x, y)$ are depicted.

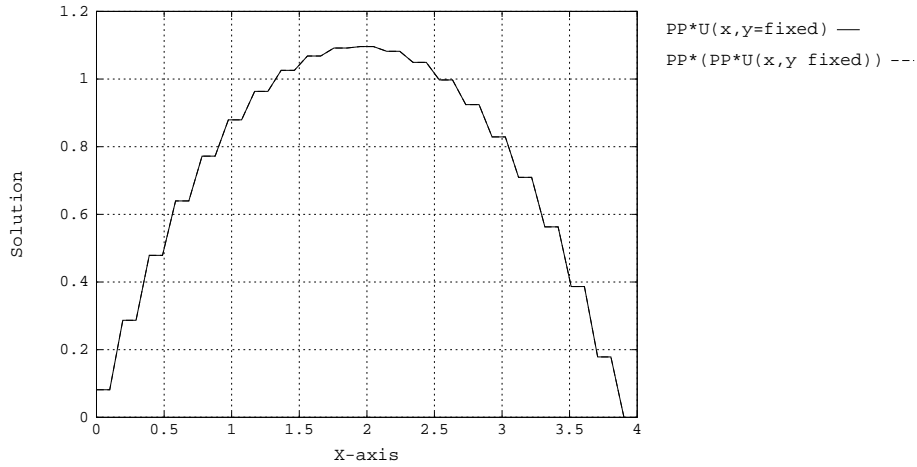


Figure 6: Sketch of $S_h S_h = S_h$ applied on a real function $u(x, y)$. Presentation of a cut ($y = 0$) of $S_h u$ (line) and $S_h S_h u$ (dashes), where the operator S_h is the composition of the operators $I_H^h I_H^H$.

From the definition $T_h = Id_h - S_h$, we deduce that :

$$T_h T_h = (Id_h - S_h)(Id_h - S_h) = Id_h - S_h = T_h$$

and

$$S_h T_h = S_h - S_h S_h = 0 \quad \square$$

Let also demonstrate that \bar{S}_h and \bar{T}_h are orthogonal projection operators :

$$\bar{T}_h \bar{T}_h = A_h^{-1} T_h A_h A_h^{-1} T_h A_h = A_h^{-1} T_h A_h = \bar{T}_h$$

$$\bar{S}_h \bar{S}_h = A_h^{-1} S_h A_h A_h^{-1} S_h A_h = A_h^{-1} S_h A_h = \bar{S}_h$$

$$\bar{S}_h \bar{T}_h = A_h^{-1} S_h A_h A_h^{-1} T_h A_h = A_h^{-1} S_h T_h A_h = 0 \quad \square$$

5 Numerical experiments

Results have been obtained on regular square meshes. In the first section, a fine square mesh with 1681 nodes is used and agglomeration method provides four coarser meshes. In the second section, we present a mesh-independent convergence rate on three fine meshes (1681, 6561 and 9409 nodes) and in the last one, AMLP method has been used in the case of an optimum design problem, the optimization of a 2D nozzle in Euler flow.

5.1 Residual convergence

With this new approach of multilevel method, we can apply a conjugation method on the residual, because it depends on all the levels in only one step iteration ; all the frequencies are reached. We use a Polak-Ribière conjugation, as described in [1], and a new descent direction d^α is found :

$$d^\alpha = Res^\alpha + \frac{\langle Res^\alpha, Res^\alpha - Res^{\alpha-1} \rangle}{\langle Res^{\alpha-1}, Res^{\alpha-1} \rangle} d^{\alpha-1}$$

where Res^α , the residual of the AMLP method, has been defined in Section 2 and it is normalized by :

$$Res^\alpha = \frac{Res^\alpha}{Res^0}.$$

Figure 7-a presents the convergence history of cost functional J computed with both methods. When using smoothing, the minimum of J is reached 3 times faster with AMLP method. Without smoothing, it is reached at the same time. If we examine the first iteration solutions obtained with both methods, Figure 7-b shows that the AMLP method provides a better first iteration solution than multilevel with V-cycles. As all the frequencies are reached in one iteration, the converged solution is faster approached.

In Figure 8, convergence of the residual has been evaluated with and without smoothing. The ρ_i 's have been chosen twice and fourth greater on each level, and we deduce, experimentally, the same conclusion as in Section 3, with two-grid Fourier analysis. When not using smoothing, the convergence of the residual is better with steps twice larger, and when using smoothing, it is better to use steps four times larger.

The multilevel method with V-cycle strategy (see e.g. [4]) has been compared with the new approach of multilevel in Figure 9. When comparing optimization iterations, the new method is 4 times faster with smoothing and about twice faster without smoothing.

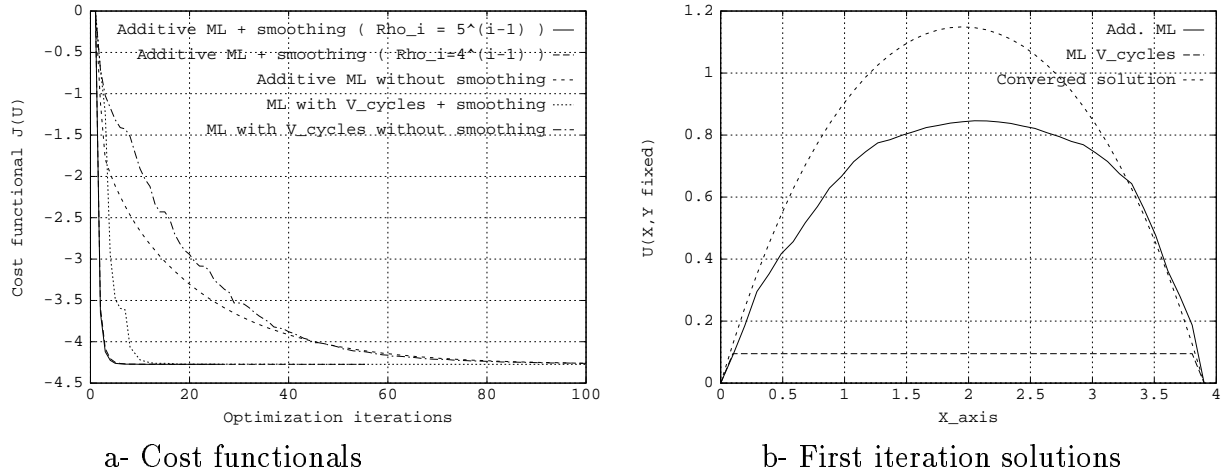


Figure 7: Comparison of cost functionals with AMLP method (with smoothing or not) and ML method with V-cycle strategy (with smoothing or not). Comparison of first iteration solutions (obtained with both methods) and converged solution.

5.2 Mesh-Independent Convergence Rate

We note on Figure 10-a a mesh-independent convergence rate with smoothing ($\rho_i = 4^{i-1}$) and simple gradient. With conjugate gradient and smoothing, the option $\rho_i = 4^{i-1}$, does not involve mesh-independent convergence rate (Figure 10-b). However, when using two-grid Fourier analysis with smoothing, we have seen that the step on the coarse level should be 5 times greater than the step on the fine one. In Figure 10-c, the independent convergence of the mesh appears.

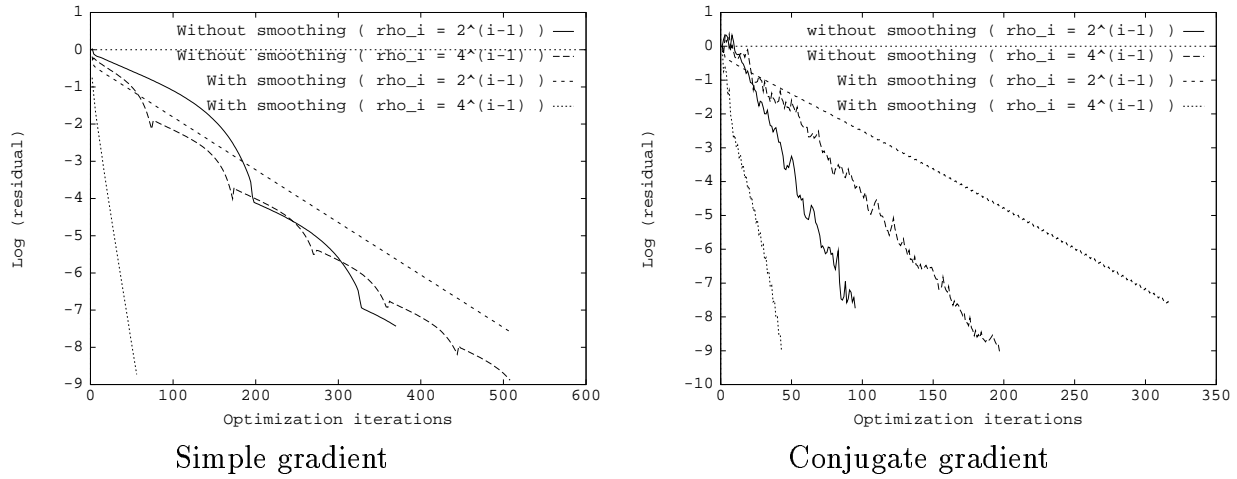


Figure 8: *Convergence of the residual with and without smoothing.*

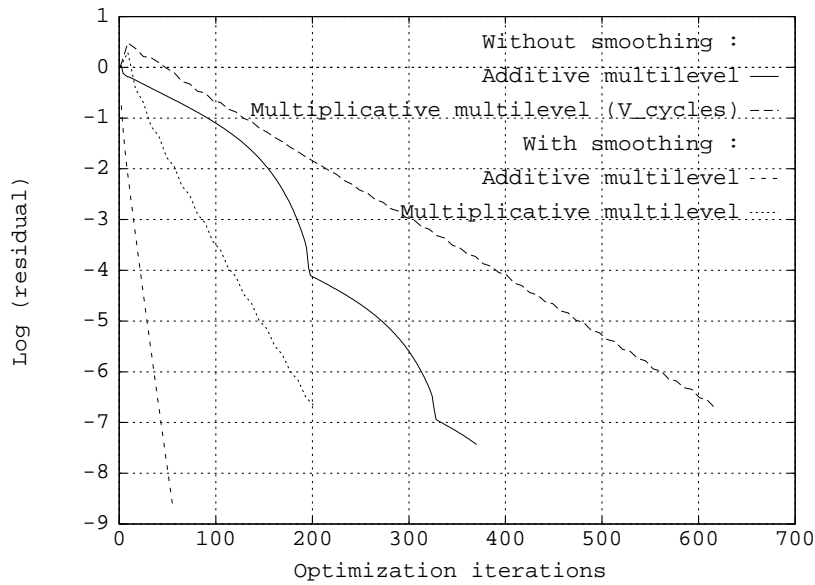
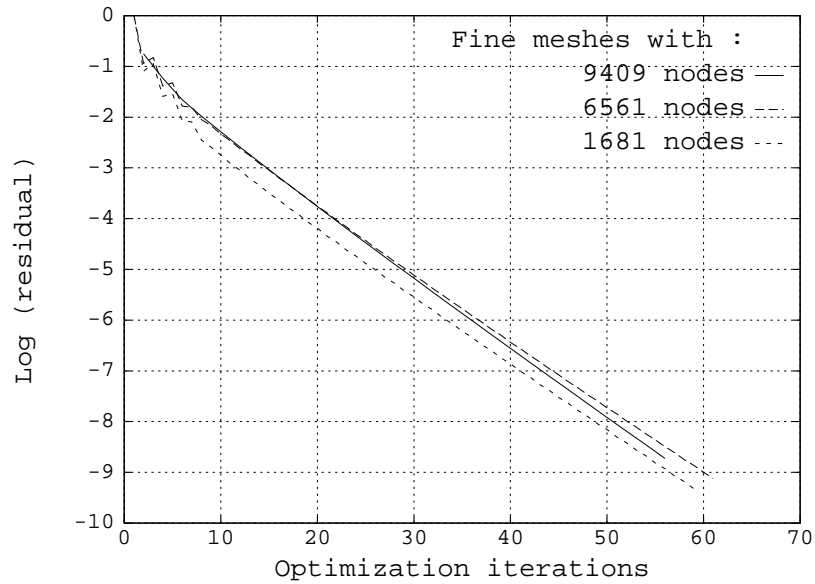


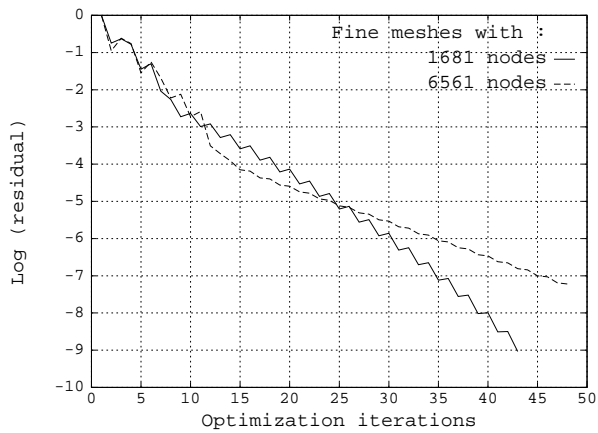
Figure 9: *Simple gradient : comparison between additive multilevel and multiplicative multilevel (with V-cycles and 1 iteration on each level).*

5.3 AMLP method applied to Optimum Design inverse Problem

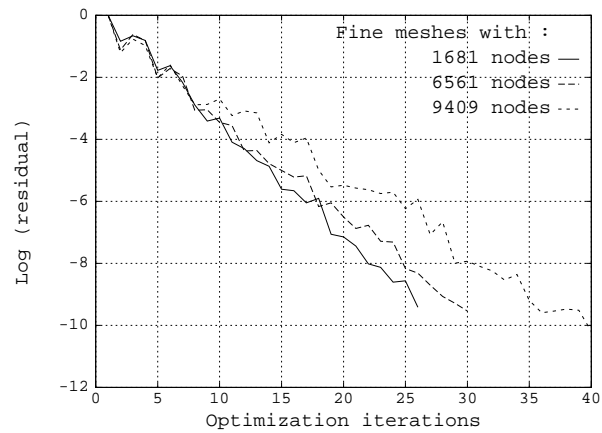
In [10], a one-shot method was applied to the problem of shape optimization of a nozzle in a 2D Euler flow. This method was combined to the multilevel



a- Simple gradient



b- Conjugate gradient with smoothing
and $\rho_i = 4^{i-1}$



c- Conjugate gradient with smoothing
and $\rho_i = 5^{i-1}$

Figure 10: Mesh-independent convergence rate on three fine square meshes : 1681, 6561 and 9409 nodes.

method with V-cycle strategy and results were very efficient. We try now to

test the one-shot combined with the AMLP method.

Results are not satisfying. Cost functional decreases faster than the one obtained with complete solution of the state and adjoint-state equations, but slower than the one of the one-shot method combined with Multilevel with V-cycle strategy (Figure 11). In fact, it is because we no more work with a descent direction, which is very difficult to adjust the optimal step ρ_{opt} with the steps ρ_i on each level. We recall that the step-length ρ_{opt} is not automatically calculated in this One-Shot method.

If we consider the complete solution of the linear systems, as we get a descent method, the optimal step-length ρ_{opt} is calculated at each iteration with an interpolation rule and ρ_i 's are chosen four times greater on coarser levels ($\rho_1 = 0.0625, \rho_2 = 0.25, \rho_3 = 1$). Figure 12 presents the convergence history of the cost functional with AMLP method. Results are convincing. Successive shapes are given on Figure 13. In Figure 14 first iteration profiles are depicted for complete solution on the fine level and complete solution with AMLP method. We note that the AMLP profile is a better approximation of the desired shape. High frequencies seen on the boundaries have been smoothed.

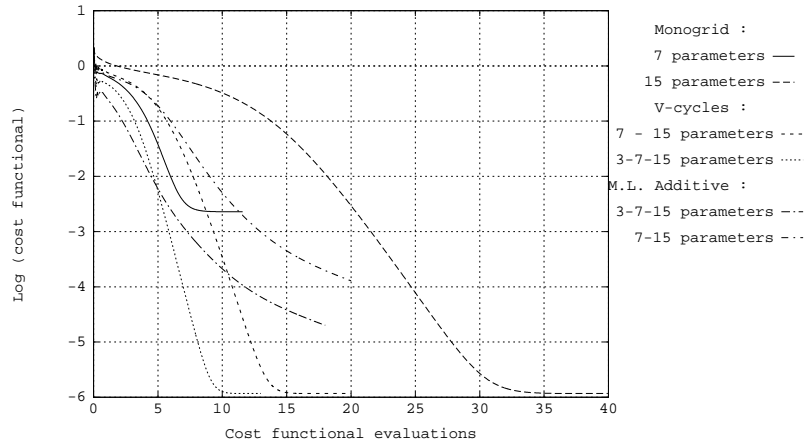


Figure 11: *One-Shot combined with ML method with V-cycle strategy and One-shot combined with AMLP method. For the first approach, the optimal step is fixed on each level (3-7-15 parameters) and on the second one, it is fixed on the finest level according to the ρ_i 's.*

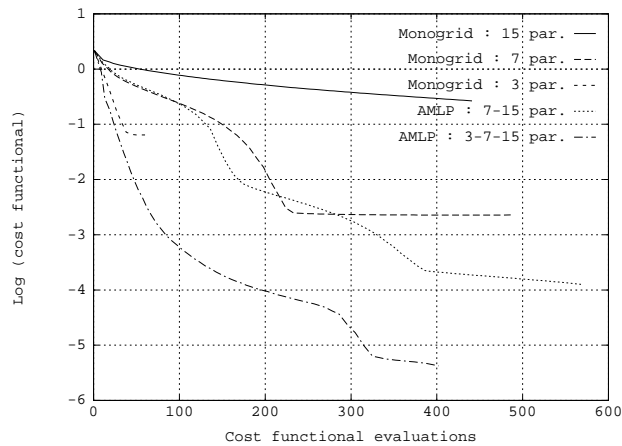


Figure 12: *Complete solution of the state and adjoint-state. Convergence history of cost functional firstly on one level (15 parameters, 7 parameters and 3 parameters) and secondly with AMLP method (7-15 parameters and 3-7-15 parameters).*

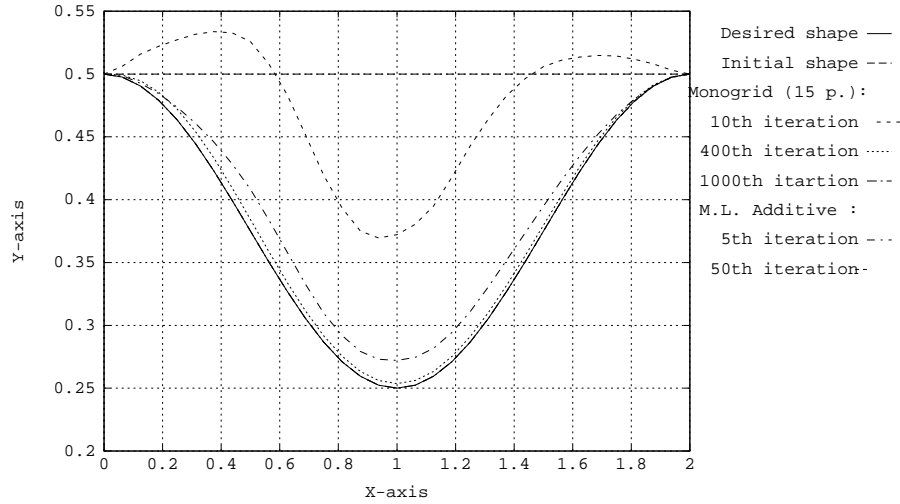


Figure 13: Complete solution of the state and adjoint-state. After 50 optimization iterations, the desired shape is completely approached by the AMLP method, while it is not yet approached with the fine grid.

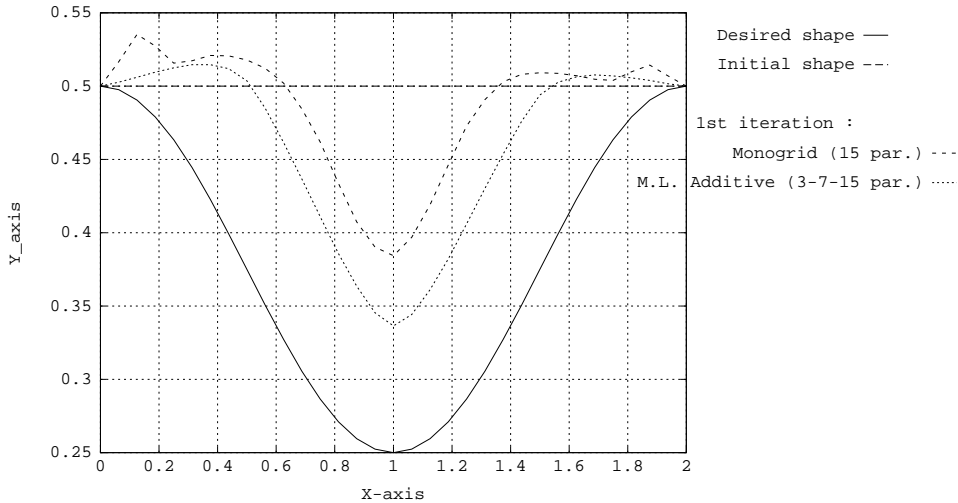


Figure 14: Solution after one optimization iteration. AMLP method gives a better convergence to the desired shape and high frequencies seen with the fine grid are smoothed with the AMLP method (work with 3 – 7 – 15 parameters).

6 Concluding remarks

This paper studies a multilevel method for optimization problems, when using a hierarchical parameterization with transfer operators. In recent works (see for example [4]), the multilevel method uses a V-cycle strategy where the cost functional, computed with all the components, is evaluated on the different levels and then, a lot of informations are not taken into account ; this involves some waste ; for the computation of the residual, the same problem appears. On a given level, we only smooth the component related to this level, while the others are not necessary. We infer that if this waste did not exist, the efficiency of the multilevel method would increase.

In the present additive standpoint, in order to avoid useless calculi, descent direction of the optimization problem ($\rho B^{-1}(Au - b)$) has been splitted in a sum of descent directions ($\sum_{i=fine}^{coarse} \rho_i (Au - b)_i$) on the different levels. The ρ_i 's are steps-length relaxation weighting each descent direction and $(Au - b)_i$ are the frequency components of the residual ($i = fine$ corresponds to high frequencies and $i = coarse$ corresponds to low frequencies). In one optimization iteration, all the components of the residual are attacked and it demands only one evaluation of the cost functional.

On a simplified example (Poisson equation), some theoretical results have been proposed : creation of a new splitted descent direction, construction of a hierarchical preconditioning of the same nature of matrix A , and a convergence theory for the multilevel algorithm has been proposed for a mesh-independent convergence rate.

The AMLP method has been tested on two numerical experiments : firstly, when solving a simplistic problem, solution of 2D Laplace equation by the optimization of a symmetric, positive definite cost functional. The method is very efficient in comparison with multilevel method with V-cycle strategy : the optimization iterations number has been reduced from a factor 2 without the “smoothing” operators L and L^* and a factor 4 with the “smoothing” operators. We also note a mesh-independent convergence rate on meshes of similar

topology. The second numerical experiment concerns the introduction of the AMLP method in a more difficult problem : the optimization of a nozzle in a 2D Euler flow. When solving completely linear systems (state and adjoint-state equations), the additive method is satisfying. Fewer cost functionals are evaluated. However, when solving simultaneously the linear systems (One-Shot method), the combination with the AMLP method is not as efficient as the multilevel method with V-cycle strategy.

To sum up, this new multilevel approach brings several improvements ; in particular, we can combine it with the conjugate gradient, which we could not do in the previous method. The obtained results are interesting with respect with CPU time. In the future, it could be interesting to combine this additive method with several more performant solvers and to apply it to non-symmetric problems.

Appendix 1

2-Grids Fourier Analysis for scheme (32), without smoothing.

Even components of the error :

$$U_{2j}^{n+1} = U_{2j-1}^n \frac{\rho_2 + \rho_1}{4} + U_{2j}^n \left(1 - \frac{\rho_2 + 3\rho_1}{4}\right) + U_{2j+1}^n \frac{3\rho_1 - \rho_2}{4} + U_{2j+2}^n \frac{\rho_2 - \rho_1}{4}$$

Odd components of the error :

$$U_{2j+1}^{n+1} = U_{2j-1}^n \frac{\rho_2 - \rho_1}{4} + U_{2j}^n \frac{3\rho_1 - \rho_2}{4} + U_{2j+1}^n \left(1 - \frac{\rho_2 + 3\rho_1}{4}\right) + U_{2j+2}^n \frac{\rho_2 + \rho_1}{4}$$

When using Fourier modes as defined in (26), the amplification matrix is :

$$\begin{pmatrix} \hat{U}_k^{n+1} \\ \hat{V}_k^{n+1} \end{pmatrix} = G(\Theta_k, \rho_1, \rho_2) \begin{pmatrix} \hat{U}_k^n \\ \hat{V}_k^n \end{pmatrix}$$

where :

$$G(\Theta_k, \rho_1, \rho_2) = \begin{pmatrix} g1(\Theta_k, \rho_1, \rho_2) & g2(\Theta_k, \rho_1, \rho_2) \\ g2(-\Theta_k, \rho_1, \rho_2) & g1(-\Theta_k, \rho_1, \rho_2) \end{pmatrix}$$

with :

$$\begin{cases} g1(\Theta_k, \rho_1, \rho_2) = 1 - \frac{\rho_2 + 3\rho_1}{4} + \frac{\rho_2 - \rho_1}{4} \exp(2i\Theta_k) \\ g2(\Theta_k, \rho_1, \rho_2) = \frac{\rho_2 + \rho_1}{4} \exp(-i\Theta_k) + \frac{3\rho_1 - \rho_2}{4} \exp(i\Theta_k) \end{cases}$$

Appendix 2

2-Grids Fourier Analysis for scheme (33), with smoothing.

Even components of the error :

$$\begin{aligned} U_{2j}^{n+1} = & U_{2j}^n \left(1 - \rho_1 - \frac{5}{64}(\rho_2 - \rho_1)\right) + U_{2j-4}^n \frac{1}{64}(\rho_2 - \rho_1) \\ & + U_{2j-3}^n \frac{1}{64}(\rho_2 - \rho_1) + U_{2j-2}^n \frac{1}{64}(\rho_2 - \rho_1) \\ & + U_{2j-1}^n \left(\frac{1}{2}\rho_1 + \frac{1}{64}(\rho_2 - \rho_1)\right) + U_{2j+1}^n \left(\frac{1}{2}\rho_1 - \frac{5}{64}(\rho_2 - \rho_1)\right) \\ & + U_{2j+2}^n \frac{3}{64}(\rho_2 - \rho_1) + U_{2j+3}^n \frac{3}{64}(\rho_2 - \rho_1) \end{aligned}$$

Odd components of the error :

$$\begin{aligned}
U_{2j}^{n+1} &= U_{2j}^n \left(\frac{1}{2} \rho_1 - \frac{5}{64} (\rho_2 - \rho_1) \right) + U_{2j-2}^n \frac{3}{64} (\rho_2 - \rho_1) \\
&+ U_{2j-1}^n \frac{3}{64} (\rho_2 - \rho_1) + U_{2j+1}^n \left(1 - \rho_1 - \frac{5}{64} (\rho_2 - \rho_1) \right) \\
&+ U_{2j+2}^n \left(\frac{1}{2} \rho_1 + \frac{1}{64} (\rho_2 - \rho_1) \right) + U_{2j+3}^n \frac{1}{64} (\rho_2 - \rho_1) \\
&+ U_{2j+4}^n \frac{1}{64} (\rho_2 - \rho_1) + U_{2j+5}^n \frac{1}{64} (\rho_2 - \rho_1)
\end{aligned}$$

When using Fourier modes as defined in (26), we write the amplification matrix by :

$$\begin{pmatrix} \hat{U}_k^{n+1} \\ \hat{V}_k^{n+1} \end{pmatrix} = G(\Theta_k, \rho_1, \rho_2) \begin{pmatrix} \hat{U}_k^n \\ \hat{V}_k^n \end{pmatrix}$$

where :

$$G(\Theta_k, \rho_1, \rho_2) = \begin{pmatrix} g1(\Theta_k, \rho_1, \rho_2) & g2(\Theta_k, \rho_1, \rho_2) \\ g2(-\Theta_k, \rho_1, \rho_2) & g1(-\Theta_k, \rho_1, \rho_2) \end{pmatrix}$$

with :

$$\left\{ \begin{array}{l} g1(\Theta_k, \rho_1, \rho_2) = 1 - \rho_1 - \frac{5}{64} (\rho_2 - \rho_1) + \frac{1}{64} (\rho_2 - \rho_1) \exp(-4i\Theta_k) \\ \quad + \frac{1}{64} (\rho_2 - \rho_1) \exp(-2i\Theta_k) + \frac{3}{64} (\rho_2 - \rho_1) \exp(2i\Theta_k) \\ g2(\Theta_k, \rho_1, \rho_2) = \frac{1}{64} (\rho_2 - \rho_1) \exp(-3i\Theta_k) + \left(\frac{1}{2} \rho_1 + \frac{1}{64} (\rho_2 - \rho_1) \right) \exp(-i\Theta_k) \\ \quad + \left(\frac{1}{2} \rho_1 - \frac{5}{64} (\rho_2 - \rho_1) \right) \exp(i\Theta_k) + \frac{3}{64} (\rho_2 - \rho_1) \exp(3i\Theta_k) \end{array} \right.$$

References

- [1] F. BEUX and A. DERVIEUX. A hierarchical approach for shape optimization. *Engineering Computation*, 11(1):25–48, February 1994.

-
- [2] T. CHAN and R. TUMINARO. Design and Implementation of Parallel Multigrid Algorithms. In *Proceedings of Third Copper Mountain Conference on Multigrid Methods*. S.F. McCORMICK (ed), Marcel Dekker, New-York and Basel, 1987.
 - [3] V. COUAILLIER and R. PEYRET. Etude théorique et numérique de la méthode multigrille de Ni. *La Recherche Aéronautique*, 5:285–300, 1986.
 - [4] A. DERVIEUX, J.M. MALE, N. MARCO, J. PERIAUX, B. STOUFFLET, and H.Q. CHEN. Some Recent advances in Optimal Shape Design for Aeronautical Flows. In *ECCOMAS 2nd Computational Fluid Dynamics Conference*, University of Stuttgart - Germany, September 1994.
 - [5] A. DERVIEUX, E. MORANO, M.-H. LALLEMAND, M.-P. LECLERCQ, and B. STOUFFLET. Two-Grid Analysis and non structured MG for Hyperbolics. In *Multigrid Method for Computational Fluid Dynamics - ERCIM*, INRIA-Sophia Antipolis, February 1992.
 - [6] H. GUILLARD. Convergence analysis of a multi-level relaxation method. Research report 1884, INRIA Sophia-Antipolis, Avril 1993.
 - [7] B. KOOBUS and M.-H. LALLEMAND. An additive standpoint in parallel two-level multigrid algorithm. Research report in preparation, INRIA Sophia-Antipolis, 1994.
 - [8] M.-P. LECLERCQ and B. STOUFFLET. Characteristic Multigrid Method Application to solve the Euler equations with unstructured and unnested grids. In *International Conference on Hyperbolic Problems*, Uppsala, 1989.
 - [9] N. MARCO. Solution of 2-D Poisson Equation by Multilevel Optimization on Unstructured Meshes. Research report in preparation, INRIA Sophia-Antipolis, 1994.
 - [10] N. MARCO and F. BEUX. Multilevel optimization: application to one-shot shape optimum design. Research Report 2068, INRIA Sophia-Antipolis, October 1993.
 - [11] N. MARCO and A. DERVIEUX. Some Multilevel Methods for Unstructured-Mesh CFD. In *Experimentation, Modélisation, Computation in flow, Turbulence and Combustion*. J.A. Désidéri, B.N. Chetverushkin, Y.A. Kuznetsov, J. Périaux and B. Stoufflet (Eds), J. Wiley and Son Ltd, England, 1994.



Unité de recherche INRIA Lorraine, Technopôle de Nancy-Brabois, Campus scientifique,
615 rue du Jardin Botanique, BP 101, 54600 VILLERS LÈS NANCY
Unité de recherche INRIA Rennes, Irisa, Campus universitaire de Beaulieu, 35042 RENNES Cedex
Unité de recherche INRIA Rhône-Alpes, 46 avenue Félix Viallet, 38031 GRENOBLE Cedex 1
Unité de recherche INRIA Rocquencourt, Domaine de Voluceau, Rocquencourt, BP 105, 78153 LE CHESNAY Cedex
Unité de recherche INRIA Sophia-Antipolis, 2004 route des Lucioles, BP 93, 06902 SOPHIA-ANTIPOLIS Cedex

Éditeur

INRIA, Domaine de Voluceau, Rocquencourt, BP 105, 78153 LE CHESNAY Cedex (France)

ISSN 0249-6399